Biometals (2008) 21:417–423
DOI 10.1007/s10534-007-9130-7

Spectroscopic and electrochemical characterization of cytochrome *c* encapsulated in a bio sol–gel matrix

Daniela Deriu · Sara Emanuela Pagnotta · Roberto Santucci · Nicola Rosato

Received: 27 July 2007 / Accepted: 10 December 2007 / Published online: 28 December 2007
© Springer Science+Business Media, LLC. 2007

Abstract Sol–gel technique represents a remarkably versatile method for protein encapsulation. To enhance sol–gel biocompatibility, systems envisaging the presence of calcium and phosphates in the sol–gel composition were recently prepared and investigated. Unfortunately, the low pH at which solutions were prepared (pH < 2.5) dramatically limited their application to proteins, because the acidic environment induces protein denaturation. In this paper we apply a new protocol based on the introduction of calcium nitrate to the inorganic phase, with formation of a binary bioactive system. In this case protein encapsulation results versatile and secure, being achieved at a pH close to neutrality (pH 6.0); also, the presence of calcium is expected to enhance system biocompatibility. To determine the properties of the salt-doped sol–gel and the influence exerted on entrapped biosystems, the structural and functional properties of embedded cytochrome *c* have been investigated. Data obtained indicate that the salt-doped sol–gel induces no significant change in the structure and the redox properties of the embedded protein; also, the matrix increases protein stability. Interestingly, the presence of calcium nitrate appears determinant for refolding of the acid-denatured protein. This is of interest in the perspective of future applications in biosensoristic area.

Keywords Bio sol–gel · Protein encapsulation · Cytochrome *c* · Cyclic voltammetry

D. Deriu (✉) · R. Santucci (✉) · N. Rosato
Department of Experimental Medicine and Biochemical Sciences, University of Rome "Tor Vergata", Via Montpellier, 1, 00133 Rome, Italy
e-mail: daniela.deriu@uniroma2.it

R. Santucci
e-mail: santucci@med.uniroma2.it

S. E. Pagnotta
Physics Department, University of Roma – Tre, Rome, Italy

N. Rosato
INFM Genova, Rome, Italy

Introduction

Protein encapsulation methods have recently attracted great attention in view of the high potentialities they offer for the development of new materials to be employed in biotechnological area. The sol–gel technique represents a remarkably versatile method for protein encapsulation, since it provides the opportunity to work with (i) material modifiable with polymer additives and redox compounds (of interest for developing electrochemical sensors); (ii) transparent and inert samples (important for the construction of optical sensors); (iii) sol–gel matrices characterized by tuneable pore size and distribution (which permit free diffusion of ions and small molecules, but retain macromolecules entrapped in the silica network) (Avnir et al. 1994; Gill and

Ballesteros 2000; Jin and Brennan 2002; Gupta and Chaudhuri 2007). Interestingly, protein entrapment in sol–gel is achieved at room temperature and the adopted procedure does not alter protein structure, although the alcohol produced during sol–gel formation may potentially induce protein denaturation (Dave et al. 1997; Das et al. 1998). As matter of fact, sol–gel-entrapped proteins exhibit higher stability and react more promptly with exogenous reagents than soluble proteins (Dunn et al. 1998).

Nowadays, protocols concerning protein encapsulation into a sol–gel matrix are well established. The synthesis of the inorganic matrix (sol phase) generally starts with the partial (or complete) acid- (or base-) catalyzed hydrolysis of a precursor as, for example, the tetramethyl-orthosilicate (TMOS). To enhance sol–gel biocompatibility, a new protocol envisaging the presence of calcium and phosphates in sol–gel composition was recently appointed, and the properties of the ternary bio-gel (composed by calcium nitrate, phosphoric acid, and TMOS) were analyzed (Sepulveda et al. 2002; Sarapanavan et al. 2003; Balamurugan et al. 2006; Vallet-Regi et al. 2006). A dramatic limit to application of ternary biogels is represented by pH (<2.5), which often induces protein denaturation.

In this paper, we apply a new protocol based on the introduction of calcium nitrate to the inorganic phase with formation of a bioactive binary system (calcium is considered fundamental for biocompatibility). With respect to ternary bioactive systems, this procedure brings about several advantages as the possibility to achieve protein entrapment at a pH close to neutrality (i.e., pH 6.0). This avoids undesired events as protein unfolding or, in the case of myoglobin and horseradish peroxidase, release of the prosthetic group once the protein is mixed with sol–gel. Thus, this procedure renders protein encapsulation more versatile and secure.

The properties of the calcium nitrate-doped sol–gel matrix (that we shall call here bio sol–gel) have been defined by investigating the influence exerted by the matrix on structure and functionality of an embedded protein. Cytochrome *c* (cyt *c*) was chosen as reference system. This single chain hemoprotein, which acts as electron carrier in mitochondria (Moore and Pettigrew 1990; Meyer 1996), is composed of 104 aminoacidic residues and shows three major and two minor α-helices in the structure. The prosthetic group is covalently bound by two thioether bridges to two cysteine residues (Cys14 and Cys17), while His18 and Met80 are the axial ligands of the heme iron under physiological conditions. The protein high-resolution X-ray structure of cyt *c* has been solved (Bushnell et al. 1990) and its properties in solution determined (Qi et al. 1996; Banci et al. 1997; Milne et al. 1998). The relatively high stability together with some peculiar properties, as the rapid and fully reversible acid-induced unfolding process, render cyt *c* an ideal model system for studies aimed (as the present) to determine the influence of solid matrices on the properties of entrapped proteins. Results shown in the present paper provide new insights on the potential offered by biocompatible sol–gels for future application in biotechnology.

Materials and methods

Chemicals

Horse heart cytochrome *c* (type VI) and calcium nitrate, $[Ca(NO_3)_2 \cdot 4H_2O]$ were from Sigma (St Louis, USA) and were used without further purification. TMOS was from Fluka. All reagents used were of analytical grade.

Samples preparation

Protein solutions were prepared by dissolving a proper amount of cyt *c* in 50 mM Tris–HCl buffer, pH 7.0, in the absence and in the presence of 0.6 M calcium nitrate tetra-hydrated. Protein concentration was 25 μM for cyclic voltammetry measurements and 10 μM for absorption and CD measurements. Protein concentration was estimated using a $\varepsilon_{408} = 106\ mM^{-1}\ cm^{-1}$.

Preparation of sol–gel-encapsulated cyt *c*

The sol–gel stock solution was prepared by mixing in an ice-bathed flask 3.34 ml of bi-distillated water, 3.56 ml of a TMOS solution and 0.2 ml of a 0.04 M HCl solution. The mixture was kept under stirring until the sol phase was formed. Then, 3.56 ml of a salt solution (formed by adding 1.68 g of $Ca(NO_3)_2$

to 3.34 ml of bidistilled water and 0.2 ml of 0.04 M HCl) were added to the TMOS solution. During the sol preparation, hydrolysis and condensation of TMOS were catalysed by HCl. The sol–gel composition is shown in Table 1.

Cyt *c* was entrapped in the sol–gel by adding the sol phase to a buffered protein solution (50 mM Tris–HCl buffer, pH 7.0) at a 2:3 (v/v) ratio. The gel phase formed in a relatively short time, estimated in 10 min. for pure SiO_2 and 20 min. for salt-modified (CaO–SiO_2) sol–gel. The wet gels were then stored at 4°C.

Acid-induced unfolding of sol–gel-entrapped cyt *c* was achieved by adding 2 ml of a HCl solution, pH 1.5, in the cell containing the encapsulated protein. To follow the reverse process (i.e., protein refolding), the HCl solution was replaced by 2 ml of a 50 mM Tris–HCl buffer, pH 7.2.

Circular dichroism measurements

The CD measurements were carried out in the Soret region (380–450 nm) using a Jasco J-710 spectropolarimeter equipped with a PC as a data processor. The molar ellipticity (deg cm^2 $dmol^{-1}$) is expressed as $[\theta]$, on a molar heme basis.

Electronic absorption measurements

Electronic absorption spectra were recorded using a Perkin–Elmer spectrophotometer, model Lamba 18. One-centimeter path-length cells were used for the spectroscopic measurements.

Dc cyclic voltammetry (CV) measurements

Dc cyclic voltammograms were run in (a previously degassed) 20 mM phosphate buffer pH 7.0, containing 0.1 M $NaClO_4$. In the electrochemical cell, the anaerobic environment was maintained by a gentle flow of high-purity grade N2 just above the surface of the buffer solution, for ~20 min. A chemically modified pyrolytic graphite (PG) electrode (3 mm diameter; Amel) was the working electrode, a saturated calomel electrode (Amel) was the reference and a Pt ring the counter-electrode. An Amel 433/W multipolarograph interfaced with a PC as data processor was employed for CV measurements. The potentials reported in the text are referred to the Normal Hydrogen Electrode (NHE). The procedure adopted for electrode modification is summarized as follows: a GP electrode, previously polished with a fine emery paper and alumina powder and sonicated for 20 s, was coated with 5 µl of a 50 µM cyt *c* solution. Immediately later, the electrode was covered with 5 µl of a doped-sol–gel solution and let to dry for 24 h at room temperature. Then, the chemically modified electrode was ready for voltammetric measurements.

Table 1 Chemical composition of bio sol–gel determined by elementary analysis on single samples

Elements	Bio sol–gel (%)	Sol–gel (%)
N	3.6	0.3
C	0.7	1.1
H	1.6	1.4

Results and discussion

Structural properties of embedded cyt *c*

Addition of calcium nitrate (1 M final concentration) to soluble cyt *c* at neutral pH produces no significant change in the absorption spectrum of the protein (not shown), suggesting that the protein is not sensibly influenced by the salt. Acidification affects the absorption spectrum of soluble cyt *c*; as shown in Fig. 1, the Soret band (which is sensitive to the spin state of the heme-iron and to the nature of the axial ligands) blue-shifts from 410 to ~394 nm, indicating full protein unfolding (Goto et al. 1990). Conversely, in the presence of calcium nitrate the Soret band blue-shifts from 410 to ~401 nm, consistent with partial protein denaturation. This is supported by the absorption spectra illustrated in the inset of the figure: the 620-nm absorption band, ascribed to high spin (denatured) forms and clearly observable at acid pH, is weaker in the presence of salt. Taken together, these data suggest that the salt opposes full protein unfolding; an equilibrium between (at least) two distinct forms, a fully unfolded high spin form and a compact non-native low spin form, is observed in solution. In agreement with previous reports, we assume the latter being the A state of cyt *c*, a non-native compact form

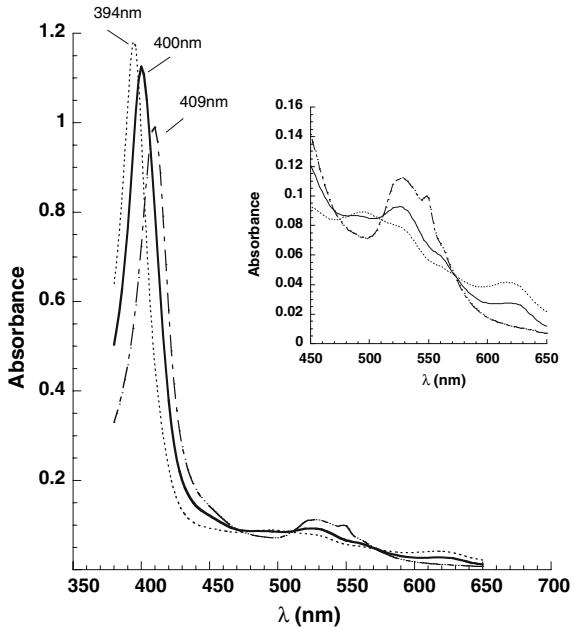

Fig. 1 Electronic absorption spectrum of acid-denaturated cytochrome *c* (pH 1.5) recorded in the absence (*dashed line*) and in the presence (*solid line*) of 1 M calcium nitrate. Insert: The same spectrum, shown in expanded scale, in the 450–650 nm wavelength range. The optical spectrum of the native protein (*dash–dot line*) is shown for comparative purposes

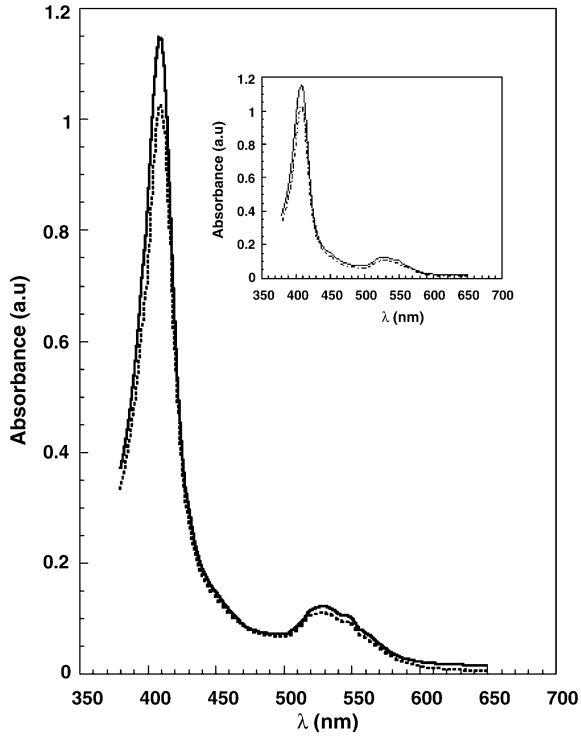

Fig. 2 Electronic absorption spectrum of cyt *c* encapsulated in bio (i.e., calcium nitrate-doped) sol–gel (*solid line*). The optical spectrum of the native protein (*dotted line*) is shown for comparison. Experimental conditions: 50 mM Tris–HCl buffer, pH 7.0; the temperature was 25°C. In the inset, the electronic absorption spectrum of cyt *c* encapsulated in bio (*solid line*) and in pure (*dotted line*) sol–gel are compared

with molten globule character (Goto et al. 1990; Jeng et al. 1990; Santucci et al. 2000). The acidic transition proved to be fully reversible.

As shown in Fig. 2, at neutral pH the absorbance and CD spectra of the encapsulated protein are almost indistinguishable from those of soluble cyt *c*, indicating (in agreement with previous results, Ellerby et al. 1992; Savini et al. 1999; Droghetti and Smulevich 2005) that the entrapped protein retains a close-to-native conformation. The slightly higher absorbance Soret spectrum shown by the embedded protein may result from the interaction (of polar nature) between protein and methanol forming during sol–gel preparation. The protein-embedding bio sol–gels (prepared as monoliths) here investigated, were homogeneous, stable, and crack-free.

The acid-induced denaturation of sol–gel-entrapped cyt *c* was investigated following the shift of the Soret absorption band as a function of time. Unlike soluble cyt *c*, the embedded protein undergoes full unfolding both in the absence and in the presence of salt (spectra not shown). Thus, the salt is unable to prevent denaturation of entrapped cyt *c*, perhaps because involved in bio sol–gel reticulation. The unfolding profile of the immobilized protein is shown in Fig. 3; with respect to soluble cyt *c* (which unfolds within few seconds both in the absence and in the presence of salt, not shown), the encapsulated protein requires longer time to unfold. However, the denaturation kinetics is fastened by calcium nitrate; this may be ascribed to two distinct factors: (i) the highly crowded system created by small pores in the salt-doped matrix (which is characterized by longer condensation times with respect to the salt-free matrix), and (ii) the high salt concentration that significantly reduces the protein-silica electrostatic interactions, with consequent protein destabilization. Cyt *c* and silica have in fact opposite net charge around neutrality, the former showing an isoelectric point, IP = 10.0, while the latter an IP = 2.1.

Figure 4 illustrates the refolding kinetics of acid-denatured cyt *c* in bio sol–gel, after that the acidic

solution was replaced by 50 mM Tris–HCl buffer, pH 7.0. The process was followed monitoring the red-shift of the Soret absorption band, which required ~250 min to recover the wavelength maximum typical of the native state ($\lambda = 408$ nm). The transition revealed to be fully reversible. By contrast, acid-denatured cyt *c* embedded in pure (salt-free) sol–gel is unable to refold even after 20 days, as shown in the inset of the figure. Thus, collapse of the embedded protein into the native conformation is facilitated by salt. CD Soret spectra, illustrated in Fig. 5, support the absorbance data: the negatively charged 416 nm-dichroic band, typical of the native protein, is almost fully recovered in bio sol–gel, while no spectral change is detected for acid-denatured cyt *c* embedded in pure sol–gel.

On the whole, our data show that calcium nitrate plays a critical role in influencing the unfolding/refolding process of sol–gel-embedded cyt *c*. In particular, the observation that the acid-denatured protein refolds only in the presence of calcium nitrate reflects the general tendency of salts to facilitate collapse of unfolded proteins into a compact state

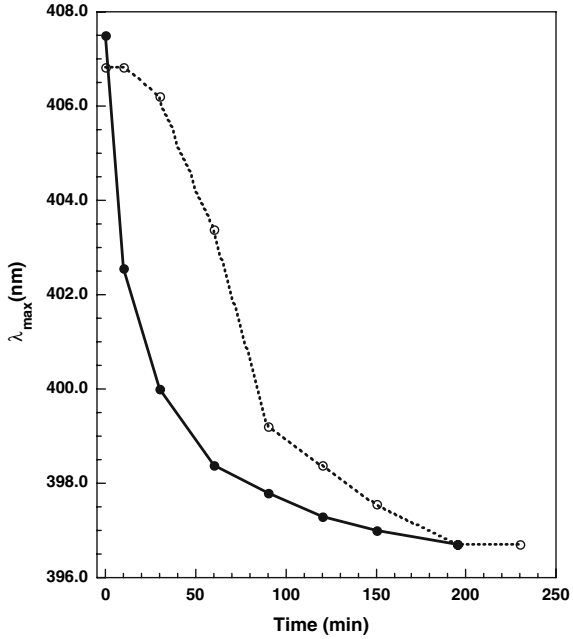

Fig. 3 Acid-denaturation kinetics of cyt *c* encapsulated in pure (*open circles*) and in bio sol–gel matrix (*solid circles*). The process was followed determining the blue-shift of the Soret absorbance band as a function of time after acidification (see text for more details). The temperature was 25°C

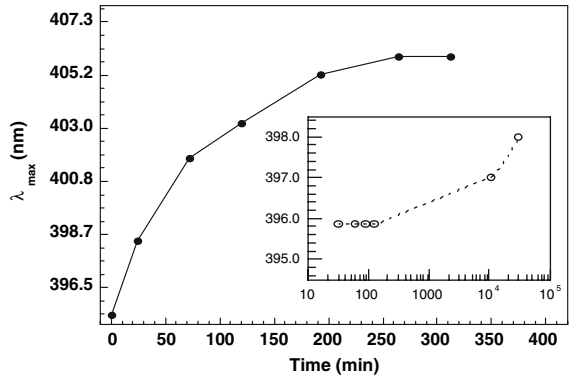

Fig. 4 Renaturation kinetics of cyt *c* encapsulated in bio sol–gel. The process was investigated by following the shift of the Soret band maximum as a function of time, after that the acid solution had been substituted with 50 mM Tris–HCl buffer, pH 7.0. The encapsulated protein fully recovers the native signal ~300 min after the change of solution occurred. The inset shows the same experiment carried out on cyt *c* encapsulated in pure sol–gel. In this case, the protein doesn't recover the native signal even after 20 days

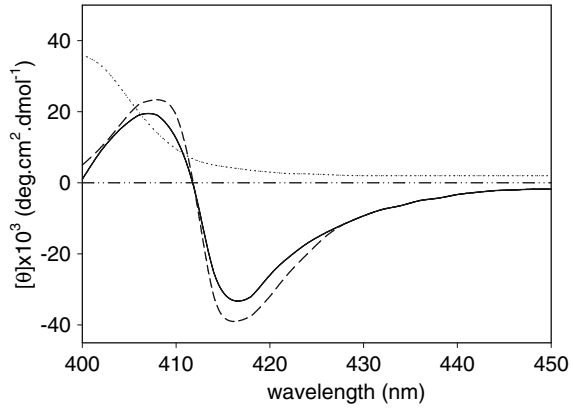

Fig. 5 Soret CD spectrum of acid-denatured cyt *c* entrapped in pure (……..) and bio (————) sol–gel, recorded after 5 h from immersion in 50 mM Tris–HCl pH 7.0. The CD spectrum of the native protein (- - - - - - -) is shown for comparison. Note that the CD spectrum of the protein embedded in pure sol gel is identical to that of the acid-denatured protein. The temperature was 25°C

(Goto et al. 1990; Jeng et al. 1990; Santucci et al. 2000).

Since data of Figs. 3 and 4 were obtained in the presence of a limited volume of solvent (i.e., that contained in a cuvette, which may affect the rate of the unfolding/refolding process), we carried out additional experiments on bio sol–gel samples soaked in a Falcon tube containing 20 ml of solution. We found that in excess of solvent the protein unfolds

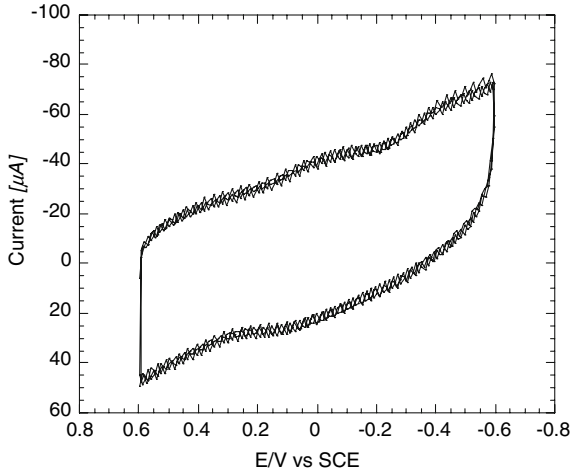

Fig. 6 Cyclic voltammogram of sol–gel-entrapped cyt *c* immobilized on a PG electrode, run in 50 mM phosphate buffer, pH 7.0, at 25°C. The scan rate was 1.5 V s^{-1}

more rapidly. The Soret absorbance band blue-shifts from 410 to 394 nm within 120 min (rather than 150–200 min), indicating that the amount of solvent influences the diffusion rate inside the cyt *c*-entrapping sol–gel network. Finally, (similarly to sol–gels) bio sol–gels stabilize the embedded protein: 1 month after preparation, the samples stored at 4°C still appeared transparent and crack-free, and their absorption spectra were almost undistinguishable from those of fresh sol–gels.

Redox properties of embedded cyt *c*

The effect exerted by the sol–gel matrix on the functional (i.e., redox) properties of the embedded protein was determined by electrochemistry. To this issue cyclic voltammograms of the embedded protein, properly immobilized on a PG electrode, were run at pH 7.0 and 25°C (for a detailed description of electrode modification, see the "Materials and methods" section). Figure 6 shows the cyclic voltammogram run at 1.5 V s^{-1}. A well defined, quasi-reversible electrochemistry is observed; the peak-separation, ΔE_p = 200 mV, while the calculated $E_{1/2}$ = 0.244 V versus NHE, is very close to the formal redox potential determined for soluble cyt *c* at the same pH ($E_{1/2}$ = 0.255 V) (Eddowes and Hill 1979). This indicates that the embedded protein retains its native-like redox properties and that the native Met80–Fe(III) axial coordination is preserved (Ferri et al. 1996; Senn and Wuthrich 1985; Sinibaldi et al. 2001). Well defined, quasi-reversible cyclic voltammograms were obtained at scan rates ranging from 20 to 1,500 mV s^{-1}; the high scan rates reached indicate that the immobilized protein undergoes rapid electron exchange with the electrode surface. Also, the embedded system shows enhanced stability: the cyclic voltammograms run every 24 h for 7 days showed shape and signal intensity almost unchanged. This suggests that the bio sol–gel matrix not only maintains unaltered the redox potential of cyt *c*, it also exerts a protecting action by enhancing protein stability and facilitating the heterogeneous electron transfer with the electrode surface.

Conclusions

In conclusion, our data reveal that cyt *c* entrapped into a calcium nitrate-doped (bio) sol–gel matrix shows spectroscopic (an, thus, structural) properties unaltered with respect to the soluble protein. Further, the presence of the salt results critical for refolding of the acid-denatured protein into the native conformation (the process does not take place in pure, salt-missing, sol–gel). The embedded protein shows high stability: 1 month after preparation, the aged samples appear transparent and crack-free, with spectroscopic properties almost identical to those of fresh samples.

The redox potential of bio sol–gel embedded cyt *c* remains unchanged with respect to the soluble native protein, suggesting that the matrix does not alter the protein behaviour. The bio sol–gel facilitates a rapid heterogeneous electron transfer between the protein and the electrode surface and exerts a protecting action on the protein (which remains electroactive for at least 1 week after preparation). Taken together, these features open new perspectives for future application of bio-gels in biosensoristic area.

Acknowledgement Research funded in part by grants from Italian MIUR (PRIN 2004055484).

References

Avnir D, Braun S, Lev O, Ottolenghi M (1994) Enzymes and other proteins entrapped in sol–gel materials. Chem Mater 6:1605–1614

Balamurugan A, Sockalingum G, Michel J, Fauré J, Banchet V, Wortham L, Bouthors S, Laurent-Maquin D, Balossier G (2006) Synthesis and characterisation of sol gel derived bioactive glass for biomedical applications. Mater Lett 60:3752–3757

Banci L, Bertini I, Gray HB, Luchinat C, Reddig T, Rosato A, Turano P (1997) Solution structure of oxidized horse heart cytochrome *c*. Biochemistry 36:9867–9877

Bushnell GW, Louie GV, Brayer GD (1990) High-resolution three-dimensional structure of horse heart cytochrome *c*. J Mol Biol 214:585–595

Das TK, Khan I, Rousseau DL, Friedman JM (1998) Preservation of the native structure in myoglobin at low pH by sol–gel encapsulation. J Am Chem Soc 120:10268–10269

Dave BC, Miller JM, Dunn B, Valentine JS, Zinc JI (1997) Encapsulation of proteins in bulk and thin film sol–gel matrices. J Sol–Gel Sci Technol 8:629–634

Droghetti E, Smulevich G (2005) Effect of sol–gel encapsulation on the unfolding of ferric horse heart cytochrome *c*. J Biol Inorg Chem 10:696–703

Dunn B, Miller JM, Dave BC, Valentine JS, Zink JI (1998) Strategies for encapsulating biomolecules in sol–gel matrices. Acta Mater 46:737–741

Eddowes MJ, Hill HAO (1979) Electrochemistry of horse heart cytochrome *c*. J Am Chem Soc 101:4461–4464

Ellerby LM, Nishida CR, Nishida F, Yamanaka SA, Dunn B, Valentine JS, Zink JI (1992) Encapsulation of proteins in transparent porous silicate glasses prepared by the sol–gel method. Science 255:113–115

Ferri T, Poscia A, Ascoli F, Santucci R (1996) Direct electrochemical evidence for an equilibrium intermediate in the guanidine-induced unfolding of cytochrome *c*. Biochim Biophys Acta 1298:102–108

Gill I, Ballesteros A (2000) Bioencapsulation within synthetic polymers (part 2): non-sol–gel protein-polymer biocomposites. Trends Biotechnol 18:469–479

Goto Y, Takahashi N, Fink AL (1990) Mechanism of acid-induced folding of proteins. Biochemistry 29:3480–3488

Gupta R, Chaudhury NK (2007) Entrapment of biomolecules in sol–gel matrix for applications in biosensors: problems aand future prospects. Biosens Bioelectron 22:2387–2399

Jeng M, Englander SW, Elove GA, Roder H, Wand AJ (1990) Structural description of acid-denatured cytochrome *c* by hydrogen exchange and 2D NMR. Biochemistry 29:10433–10437

Jin W, Brennan JD (2002) Properties and applications of proteins encapsulated within sol–gel derived materials. Anal Chim Acta 461:1–36

Meyer TE (1996) Evolution and classification of *c*-type cytochromes. In: Scott RA, Mauk AG. (eds) Cytochrome *c*. A multidisciplinary approach. University Science Books, Sausalito

Milne JS, Mayne L, Roder H, Wand AJ, Englander SW (1998) Determinants of protein hydrogen exchange studied in equine cytochrome *c*. Protein Sci 7:739–745

Moore GR, Pettigrew GW (1990) Cytochromes *c*. Evolutionary, structural and physicochemical aspects. Springer, Berlin

Qi PX, Beckman RA, Wand AJ (1996) Solution structure of horse heart ferricytochrome *c* and detection of redox-related structural changes by high-resolution 1H NMR. Biochemistry 35:12275–12286

Santucci R, Bongiovanni C, Mei G, Ferri T, Polizio F, Desideri A (2000) Anion size modulates the structure of the A state of cytochrome *c*. Biochemistry 39:12632–12638

Sarapanavan P, Jones JR, Pryce RS, Henc LL (2003) Bioactivity of gel-glass powders in the $CaO–SiO_2$ system: a comparison with ternary ($CaO–P_2O_5–SiO_2$) and quaternary glasses ($SiO_2–CaO–P_2O_5–Na_2O$). J Biomed Mater Res A 66:110–119

Savini I, Santucci R, Di Venere A, Rosato N, Struckul G, Pinna F, Avigliano L (1999) Catalytic and spectroscopic properties of cytochrome *c*, horseradish peroxidase and ascorbate oxidase embedded in a sol–gel silica matrix as a function of gelation time. Appl Biochem Biotechnol 82:227–241

Senn H, Wuthrich K (1985) Amino acid sequence, heme-iron coordination geometry and functional properties of mitochondrial and bacterial *c*-type cytochromes. Q Rev Biophys 18:111–134

Sepulveda P, Jones JR, Henc LL (2002) In vitro dissolution of melt-derived 45S5 and sol–gel derived 58S bioactive glasses. J Biomed Mater Res 61:301–311

Sinibaldi F, Fiorucci L, Mei G, Ferri T, Desideri A, Ascoli F, Santucci R (2001) Cytochrome *c* reconstituted from two peptide fragments displays native-like redox properties. Eur J Biochem 268:4537–4543

Vallet-Regi M, Salinas AJ, Arcos D (2006) From the bioactive glasses to the star gels. J Mater Sci Mater Med 17:1011–1017